Functional connectivity alterations of the temporal lobe and hippocampus in semantic dementia and Alzheimer's disease

Simon Schwab[1,4], Soroosh Afyouni[1] , Yan Chen[2], Zaizhu Han[3], Qihao Guo[3], Thomas Dierks[4], Lars-Olof Wahlund[5], and Matthias Grieder[4]

1 Big Data Institute, Li Ka Shing Centre for Health Information and Discovery, Nuffield Department of Population Health, University of Oxford, Oxford, United Kingdom
2 State Key Laboratory of Cognitive Neuroscience and Learning, Beijing Normal University, Beijing, China
3 Department of Neurology, Huashan Hospital, Fudan University, Shanghai, China
4 Translational Research Center, University Hospital of Psychiatry, University of Bern, Bern, Switzerland
5 Karolinska Institute, Department NVS, Division of Clinical Geriatrics, Stockholm, Sweden

Corresponding author: Matthias Grieder, PhD, Translational Research Center, University Hospital of Psychiatry Bern, Bolligenstrasse 111, 3000 Bern 60, Switzerland. Tel.: +41 319328351; Fax: +41 319309961; E-mail: matthias.grieder@upd.unibe.ch

Keywords: semantic dementia, Alzheimer's disease, functional connectivity, temporal lobe

Abbreviations: AD = Alzheimer's disease; FC = functional connectivity; HC = healthy controls; ROI = region of interest; SD = semantic dementia

Abstract

The severe semantic memory impairments in semantic dementia have been attributed to a pronounced anterior temporal lobe atrophy and a functional disruption of this brain region. In contrast, medial and posterior temporal lobe damage is predominantly found in patients with Alzheimer's disease, and has been associated with episodic memory disturbance. Despite these seemingly distinct neuropathological signatures that correspond well with the syndrome-typical symptomatology, the hippocampal deterioration common in Alzheimer's disease and semantic dementia appears paradoxical. In attempting to gain more insight into the mutual and divergent functional alterations seen in Alzheimer's disease and semantic dementia, we assessed the differences in intrinsic functional connectivity between temporal lobe regions in patients with Alzheimer's disease (n = 16), semantic dementia (n = 23), and healthy controls (n = 17). In contrast to the majority of studies that conducted comparable analyses, we were particularly interested in connectivity alterations between functional rather than anatomical regions, and therefore used a functional parcellation of the temporal cortex. The Alzheimer's disease group showed only a single connection with reduced functional connectivity as compared to the controls. This connection was located between the right orbitofrontal cortex and the right anterior temporal lobe. In contrast, functional connectivity was decreased in the semantic dementia group in six connections, mainly involving the hippocampus, lingual gyrus, temporal pole, and orbitofrontal cortex. We identified a common pathway with semantic dementia, since the functional connectivity between the right anterior temporal lobe and the right orbitofrontal cortex was reduced in both types of dementia. This might be related to semantic impairments observed in both dementia types, and abnormal social behavior at more progressed disease stages. However, to substantiate such claims, longitudinal studies that more strongly relate clinical and behavioral outcomes to functional connectivity are needed.

Introduction

Everybody occasionally experiences difficulties in integrating past events into an accurate context — a condition classified as an episodic memory disturbance. Intact episodic memory (Tulving, 1983) requires the processing of information about chronology, place and the protagonists who were involved in an event. The capability to store and retrieve autobiographical memory is however not sufficient for an intact episodic memory: we also strongly rely on a fully functioning semantic memory. Concretely, semantic memory reflects our general knowledge about concepts such as objects, people, and words. Thus, only a sound interplay of these two memory systems, episodic and semantic memory, allows a cognitively healthy state of an individual.

Previously two initially contradicting models of the neurophysiological organization of semantic memory have been harmonized as what can be characterized as a 'cortically distributed plus semantic hub' theory (Guo et al., 2013; Mummery et al., 2000). The term "distributed" refers to the idea that regions which process semantic concepts receive multimodal input from corresponding brain regions (e.g., visual attributes from visual brain regions, tactile attributes from the sensorimotor cortex, etc.). Subsequently, these multimodal inputs from distributed cortical areas converge to so-called unitary semantic concepts in the semantic hub (McClelland & Rogers, 2003; Patterson, Nestor, & Rogers, 2007). The semantic hub was found to be localized bilaterally in the anterior temporal lobe, a region which is atrophied or hypometabolized in patients with the semantic variant of primary progressive aphasia, also known as the temporal variant of frontotemporal dementia (FTD) or semantic dementia (SD) (Hodges & Patterson, 2007; Landin-Romero, Tan, Hodges, & Kumfor, 2016; Patterson et al., 2007). In SD, the onset of gray matter atrophy occurs in the anterior temporal lobes, frequently with an asymmetry towards the more affected left hemisphere. With progression of the disease, the temporal pole and medial as well as lateral temporal areas are degenerated (Collins et al., 2017). However, the patients seem to exhibit an almost intact episodic memory, when tested non-verbally, while their semantic memory is severely deteriorated (Bozeat, Lambon Ralph, Patterson, Garrard, & Hodges, 2000; Irish et al., 2016).

In contrast to SD, patients with Alzheimer's disease (AD) show predominantly episodic memory impairments, and semantic memory deficits can only be observed to a minor degree (Blackwell et al., 2004; Mascali et al., 2018; Vogel, Gade, Stokholm, & Waldemar, 2005). AD has been described as a disconnection syndrome, that is, connections of functionally or structurally linked brain regions that are part of a network become increasingly disrupted (Seeley, Crawford, Zhou, Miller, & Greicius, 2009; Villain et al., 2010; J. Wang et al., 2013). This degenerative mechanism has been associated with the cognitive deficits of patients with AD (Liu et al., 2016; Reijmer et al., 2013; Tijms et al., 2014). A common finding in AD is that gray matter atrophy onset can be localized in the hippocampal, posterior cingulate and lateral parietal brain regions, as well as in the amygdala (Buckner et al., 2005; Poulin et al., 2011). The hippocampus forms a core region for

episodic memory encoding. However it has also been associated with semantic memory functions (Burianova, McIntosh, & Grady, 2010). In fact, Burianova and colleagues (2010) postulated that the hippocampus is part of a *common* declarative memory network, suggesting that the hippocampus has a key role in both semantic as well as episodic and autobiographical memory.

The properties of functional systems, as for example Burianova and colleagues' proposed declarative memory network, are commonly assessed by the use of a resting-state functional connectivity (FC) analysis. The resting-state is relatively easy to investigate experimentally and in the absence of any task, requires only a minimal effort from the participants. It has become very popular to study FC alterations in various mental disorders, demonstrating that psychiatric disorders including Alzheimer's disease exhibit abnormalities in functional brain networks (Broyd et al., 2009; Greicius, Srivastava, Reiss, & Menon, 2004; Zhang & Raichle, 2010). The human resting-state is characterized by spatially discriminate brain regions that co-activate and deactivate at a low temporal frequency (Biswal, Yetkin, Haughton, & Hyde, 1995; Raichle et al., 2001). These functional systems, or resting-state networks, are commonly assessed using blood-oxygen level dependent resting-state fMRI. The most common approach to quantify FC strength is to compute the pairwise temporal correlation between a number of regions of interest (ROIs). ROIs are a-priori selected brain regions upon which the particular research question is investigated. Alternatively, in seed-based approaches only a single ROI is defined and the voxel-wise whole brain correlations are computed. Fully data-driven approaches such as independent component analysis (ICA) require little a-priori assumptions, for example no parcellation scheme is necessary (Fox & Raichle, 2007; Smith et al., 2013). Despite these different analysis strategies, the mutual rationale of all approaches to FC is that brain regions that demonstrate a statistical interdependence are considered functionally connected (Biswal et al., 1995).

This kind of large-scale network analysis has widely been applied to clinical samples such as AD and SD. Changes of FC (i.e., decreases and increases of connectivity strengths) in AD often involve the hippocampus and the default mode network (Allen et al., 2007; Kobeleva et al., 2017; Tahmasian et al., 2015; L. Wang et al., 2006). With the progression of the disease, structural and functional connectivity distortions affect several networks, particularly those involving the parahippocampus (Brier et al., 2012; Liu et al., 2016). In SD, FC appears to be deteriorated in regions either affected by or proximate to the core of atrophy, located in regions such as the temporal pole, anterior middle temporal gyrus, inferior temporal gyrus, and insula (Agosta et al., 2014; Ding et al., 2016; Farb et al., 2013; Hodges & Patterson, 2007). Furthermore, reduced FC of the anterior temporal lobe with various cortical regions was also found in SD (Guo et al., 2013).

Considering these findings as well as the distinct pathology of AD and SD, it is likely that the neuronal loss of hippocampal cells that results in gray matter atrophy certainly affects the functional networks in a way that generates episodic memory deficits. Temporal pole atrophy alone might not be necessary (but is sufficient) to lead to semantic impairment. La Joie et al. (2014) identified the hippocampus as the 'main

crossroad' between brain networks that are disrupted in AD and SD. Despite this growing body of research, the common and divergent changes of FC among regions of the temporal lobes in AD and SD are not fully understood. A caveat when interpreting the existing literature is the common use of anatomical/structural parcellation instead of a functional parcellation to study FC. Functional parcellations have the advantage that the resulting functional ROIs are homogeneous, i.e., the voxels have similar time courses. On the other hand, parcellations based on brain structure can merge the time series across functionally different areas which can be problematic (Margulies et al., 2007).

This study aimed at disentangling FC alterations of the temporal lobe in AD and SD using a refined division of temporal subregions: sixty-six functional regions of interest (ROIs) of the temporal lobes from a functional atlas (Craddock, James, Holtzheimer, Hu, & Mayberg, 2012). In contrast to numerous previous studies, we accounted for structural changes (i.e., gray matter atrophy) in order to extract FC time series data from preserved gray matter tissue which can still be functional (Duss et al., 2014; Henke, 2010). In other words, results from the FC analysis reflect the functional reorganization of the temporal lobes affected by atrophy. We investigated the pairwise region-to-region FC between each of the 66 ROIs in three participant groups (AD, SD, and healthy elderly controls). We focused our analysis on the temporal lobes with the following rationale: first, brain regions identified as the origin of atrophy are located in the temporal lobe. Second, a 'crossroad' in FC network disruption in AD and SD was found in the hippocampus. Third, functional hubs for episodic and semantic memory can be found in the temporal lobe (as outlined above). Fourth, the strongest FC of temporal regions is located within the temporal lobes and concurs with functional networks crucial for language processing, the core clinical feature of SD (Hurley, Bonakdarpour, Wang, & Mesulam, 2015). Last, analyzing 66 temporal ROIs already leads to 2,145 pairwise correlations, which necessitates a strong adjustment for multiple comparisons to control for false positives; using an even higher number of ROIs, for example comparing 200 ROIs in the whole brain, would require an even stronger correction. Such corrections would result in a sensitivity too low to detect even substantial changes in the FC and would also involve many connections not relevant for the question addressed in this study.

A common issue with studies involving patients with SD is the small sample size due to the low prevalence and relatively difficult diagnosis. In order to overcome this to some extent, we pooled two data sets from two different recording sites (see Method section for details). Orban et al. (2018) showed in multivariate fMRI analysis the advantage of multisite fMRI-data. Their approach appears to be generalizable; however, we will address some of its limitations in the discussion section.

Even though our analysis pipeline is explorative, by calculating all the pairwise correlations of the 66 ROIs, we have the following hypotheses based on the studies described above: for the AD sample, we expected alterations of the FC in the hippocampus, parahippocampal regions, and possibly posterior temporal regions. For SD, altered FC was anticipated in the hippocampus, the fusiform gyrus, and the temporal pole.

Methods

Participants

We analyzed resting-state fMRI data from a total of 62 participants from three groups: semantic dementia (SD), Alzheimer's disease (AD), and a healthy elderly control group (HC). We examined all the functional MR data and excluded six datasets due to insufficient data quality (see data quality control). The final sample consisted of 56 participants: Twenty-three patients with SD, with a mean age (± standard deviation) of 62 ± 7.6, 16 patients with AD, mean age of 70 ± 8.5, and 17 individuals in the HC group, mean age 70 ± 3.4; see table 1 for demographics and clinical variables. Patients with SD from the Stockholm site were recruited throughout Sweden and diagnosed using the criteria of Neary et al. (1998), while patients with SD from Shanghai were recruited from Huashan Hospital in Shanghai, according to the criteria of Gorno-Tempini et al. (2011). Patients with AD were recruited at the Memory Clinic of the Geriatric Department at Karolinska University Hospital in Huddinge, Sweden. Their diagnosis was performed by expert clinicians and was in accordance with the ICD-10 criteria. The patients with AD included in this study underwent a standard clinical procedure which consisted of examinations such as structural neuroimaging, lumbar puncture, blood analyses, and a neuropsychological assessment. Further inclusion criteria for all patients was a Global Deterioration Scale lower than 6 (i.e., moderate dementia or milder) and the Cornell Depression Scale below 8. Healthy elderly controls were recruited by advertisement. Presence of medical or psychiatric disorders (other than dementia), intake of drugs affecting the nervous system, or magnetic implants, led to an exclusion from the study. All study participants provided informed consent prior to the data acquisition.

MR data

MR images were acquired on two sites: The Karolinska Institute in Stockholm, Sweden, and the Huashan Hospital in Shanghai, China.

Stockholm site

MR images were acquired with a 3T Siemens Magnetom Trio scanner (Siemens AG, Erlangen, Germany). Structural images were 3D T1-weighted magnetization-prepared rapid gradient echo (MPRAGE) images using the following parameters: TR = 1900 ms, TE = 2.57 ms, flip angle = 9°, matrix size = 256 × 256, field of view = 230 × 230 mm^2, slice number = 176 slices, slice thickness = 1 mm, and voxel size = 0.90 × 0.90 × 1 mm^3. The structural images were previously used for voxel-based morphometry and published with a different purpose and sample configuration (Andreotti, Dierks, Wahlund, & Grieder, 2017; Grieder et al., 2013).

Functional images were acquired with a 32-channel head coil, using an interleaved EPI sequence (400 volumes; 26 slices; voxel, $3 \times 3 \times 4$ mm^3; gap thickness, 0.2 mm; matrix size, 80×80; FOV, 240×240 mm^2; TR, 1600 ms; TE, 35 ms).

Shanghai site

Images were acquired with a 3T Siemens Magnetom Verio. Structural images were 3D T1-weighted magnetization-prepared rapid gradient echo (MPRAGE) images using the following parameters: TR = 2300 ms, TE = 2.98 ms, flip angle = 9°, matrix size = 240 × 256, field of view = 240 × 256 mm^2, slice number = 192 slices, slice thickness = 1 mm, and voxel size = 1 × 1 × 1 mm^3. Functional images were acquired with a 32-channel head coil, using an interleaved EPI sequence (200 volumes; 33 slices; voxel, $4 \times 4 \times 4$ mm^3; gap thickness, 0 mm; matrix size, 64×64; FOV, 256×256 mm^2; TR, 2000 ms; TE, 35 ms, flip angle 90°). The data was previously published with a different sample configuration (SD only sample) in a combined structural and functional study using a hippocampus seed region (Chen et al., 2017), as well as in a structural VBM study (Ding et al., 2016).

Preprocessing of functional scans

We performed pre-processing using SPM12 (http://www.fil.ion.ucl.ac.uk/spm). We initially set all images' origin to the anterior commissure, and then performed slice-time correction, realignment, coregistration, normalization to MNI space ($2 \times 2 \times 2$ mm^3), and smoothing (full width half maximum [FWHM]; 8 mm). Time-series data was high-pass filtered (1/128 Hz) and we regressed out 14 nuisance parameters (6 movement parameters and its first derivative, white matter, and CSF).

We inspected the spatio-temporal quality of each scan by comparing the slow and fast components of the data using DSE (Dvar, Svar & Evar) decomposition (Afyouni & Nichols, 2018). The DSE technique decomposes the dataset into three main components: fast, which is the squared mean difference; slow, which is the squared mean averages, and Evar, which refers to the sum of squares of the two ends of the time series. Subjects with remarkably high divergence (>75%-tile) between Dvar and Svar components were removed, as suggested in Afyouni & Nichols (2018). Therefore, we removed one SD and three HC datasets from the analysis. We further excluded two AD subjects, as more than 20% of their DVARS data-point were found to be corrupted. The remaining subjects were scrubbed as suggested by Power et al. (2012). Thus, altogether we excluded six datasets (9.7%) due to poor data quality. We re-run the diagnostics on the final sample and we found no difference between groups regarding the DSE diagnostics (one-way ANOVA, all $p > 0.05$).

Functional connectivity analysis

We used a functional atlas of 66 nodes of the temporal cortex. The reason to use a functional atlas is that anatomical atlases do not directly map to functional units and contain functionally heterogeneous regions. Instead, the nodes of an atlas should represent functionally homogeneous regions and should further match the functional segregation present at the individual level. The functional parcellation we used is based on resting-state fMRI data which was clustered into spatially coherent regions of homogeneous FC and was evaluated in terms of the generalizability of group level results to the individual (Craddock et al., 2012) . From the 200 nodes, we used a subset of 66 temporal regions that covered at least 5% or more of one of the following temporal structures: the superior temporal cortex, the middle temporal cortex, the inferior temporal cortex, the temporal pole, the hippocampus, the parahippocampal cortex, the lingual gyrus, the amygdala, the insular cortex, and the fusiform gyrus; these 66 ROIs are shown in supplementary figure 1. We extracted the mean time-series from the gray matter (probability > 0.70) of these ROIs, resulting in 66 time-series per subject. To address motion and physiological confounds which are global in nature, we applied global signal regression to the time series (Chang & Glover, 2009; Power et al., 2014). We created a pair-wise correlation matrix and transformed the correlation coefficient to Z scores by Fisher's transformation. We conducted a one-way ANCOVA for each node pair (2145 tests) to test the null hypothesis of no difference between the three groups with age as a covariate. We found 318 significant edges that showed a group effect (uncorrected, $p < 0.05$), and after accounting for multiple comparisons, seven edges showed a significant group effect (FDR corrected, $p < 0.05$).

Voxel-based morphometry analysis

We additionally performed voxel-based morphometry (VBM) analysis to quantify gray matter loss in the patients from the anatomical T1 images. VBM is a voxel-wise comparison of the local amount of gray matter volume between two groups (Ashburner & Friston, 2000). We performed the following processing steps: spatial registration to MNI space (voxel size: 1.5 x 1.5 x 1.5 mm^3) and tissue segmentation, bias correction of the intensities, smoothing of the GM images with 8 mm FWHM, and modulation by scaling with the total volume so that the resulting mount of gray matter in the modulated images remains the same as in the native images. In other words, this step removes the introduced bias from the registration of different brain sizes to MNI space. The Stockholm sample was registered to the European brain template, the Shanghai sample to the East Asian brain template. We used the "Computational Anatomy Toolbox" CAT12 (Gaser & Dahnke, 2016) and SPM12 (Friston, Ashburner, Kiebel, Penny, & Nichols, 2007) for the VBM analysis. Statistical inference was performed with the "Statistical NonParametric Mapping" software SnPM13 using non-parametric permutation/randomization two-sample t-tests with a voxel-wise family-wise error correction (FWE) of 0.05. We performed two t-tests and compared the HC group vs. the

SD group, and the HC group vs. the AD group. Unlike in the analyses of the functional data where we excluded six datasets, the structural T1 scan from all the subjects were used in this analysis, the group sizes were HC with n = 20, AD with n = 18, SD with n = 24.

Results

We first describe the clinical presentation of the patients included in this study (see table 1 for details). From a general cognitive perspective, the MMSE indicated that the SD group was more severely demented than the AD group (Kruskal-Wallis over all groups: H = 29.5, df = 2, p < 0.001; Kolmogorov-Smirnov group-wise post-hoc tests: HC-AD Z = 1.86, p = 0.002, HC-SD Z = 2.52, p < 0.001, AD-SD Z = 1.44, p = 0.033). Focusing on semantic memory in the SD group, we observed that the impaired performance in picture naming (Boston Naming Test [BNT] for the Stockholm site, oral picture-naming for the Shanghai site) was more pronounced than in associative tasks (word-triple association for the Shanghai site, lexical decision for the Stockholm site, although these task are not fully comparable). Finally, our AD group also showed semantic deficits as compared to the healthy control group.

Next, we report the gray matter atrophy found in the patient groups, see figure 1. In the SD patients (figure 1A) we found two clusters, and atrophy was predominantly located in the left anterior medial temporal cortex, with a peak effect in the left temporal fusiform cortex (peak t-score = 14.0, df = 42; location at x = -34, y = -3, z = -36; cluster area 80.7 cm^3). In the right hemisphere, the strongest gray matter atrophy was also located in the temporal fusiform cortex (peak t-score = 10.6, df = 42; location at x = 34, y = -3, z = -34; cluster area 40.1 cm^3). In the AD patients, we found two clusters with lower GM volume in the left amygdala (peak t-score = 8.72, df = 36; location at x = -26, y = -10, z = -12; cluster area 7.23 cm^3) and right amygdala (peak t-score = 7.49, df = 36; location at x = 22, y = -3, z = -15; cluster area 7.47 cm^3), see figure 1B.

To achieve the main goal of this study, we analyzed the functional connectivity of 56 participants using 66 functional nodes of the temporal cortex and related subcortical areas (hippocampus and amygdala). Seven connections (FC between node pairs) demonstrated a significant difference between the three groups after correcting for multiple comparisons (FDR corrected, $p < 0.05$). A detailed characterization and test statistics of these seven connections are shown in table 2; the Z-values for the significant connections are depicted in figure 2. We performed post-hoc tests (Tukey HSD) for single comparisons of the three groups to investigate the particular group contrasts that drove the significant group effect (table 3). We found that most differences were related to the SD group with significant changes in all of the seven connections: SD showed lower FC in 6 out of 7 connections compared to HC, and higher FC in one connection (edge no. 2) compared to HC. This higher FC in the SD group was also significantly higher compared to the AD group. The AD group had a lower FC compared to HC in only 1 out of the 7 connections (edge 6). Comparing the two patient groups SD, versus AD, we found that SD had a significant lower FC in 4 connections (edges 3, 4, 5, 7).

We visualized the connectivity structure and connection strengths, see figure 3. The SD group generally had a much lower connectivity compared to the other two groups. An exception was the stronger contralateral connection between the right lateral inferior occipital cortex and the left posterior superior temporal gyrus (edge no. 2). The AD group showed a lower FC compared to HC between the right middle temporal gyrus and the right frontal orbital cortex (edge no. 6). A common finding in all the three groups was that the FC between the right fusiform cortex and the right inferior temporal pole was the strongest (no. 3).

Discussion

In this study, we compared functional connectivity between semantic dementia (SD), Alzheimer's disease (AD), and elderly healthy controls (HC) using a functional parcellation of 66 regions of the temporal cortex and hippocampus to investigate intra-temporal connections and connections with contralateral temporal regions. The overall picture that emerges is that between the majority of the significant nodes, SD demonstrated the most striking decrease in FC. In the AD group, most differences compared to the HC group did not reach significance. We believe that the often described disconnections found in AD were not detected in our study due to the mild progression of the disease in our AD group. One reason could be that the remaining gray matter volume in brain regions typically affected by neuronal degeneration was sufficient to maintain an intact FC to remote areas. In other words, the damage found in mild stages might affect the intra-regional processing in local neuronal populations, whereas the inter-regional (i.e., network) FC would be affected during more advanced AD progression (McDonough & Nashiro, 2014). Future studies will require larger sample sizes to demonstrate smaller changes in FC seen even with mild state impairments.

The most intriguing finding of our study for the SD group was the decreased FC between the left posterior hippocampus and left/ right lingual gyri (edges 4 and 5). These disruptions are characteristic for the neurophysiological basis of the SD patients' typical symptomatology involving an impaired semantic memory. For instance, Sormaz et al. (2017) recently showed a correlation of FC between left the hippocampus and the lingual gyrus with topographic memory, and a correlation of semantic memory performance with FC to the intracalcarine cortex, a finding consistent with our results.

Functional connectivity between the left anterior superior/ middle temporal gyrus/ insula and the left posterior middle/ superior temporal gyrus was decreased in SD compared to HC (edge no. 1). It is important to note that this is the single connection that showed an FC difference between SD and HC exclusively (i.e., a finding specific for the SD-HC group single-comparison while neither AD-HC nor AD-SD were significant). These regions are commonly associated with cross-modal integration (as is the hypothesized semantic hub) of auditory and language processing, as well as the processing of the

emotionally relevant context. Hence, this finding might reflect the severe semantic deficits in SD (see table 1) that are manifested by the loss of conceptual knowledge (Landin-Romero et al., 2016).

The single connection that showed increased FC in SD compared to the other groups (edge no. 2) was between the left posterior superior temporal gyrus/ parietal opercular cortex/ planum temporale and the right lateral inferior/ superior occipital cortex. The temporal brain areas that constitute this connection are important for early context integration of acoustically presented words (Shtyrov & Pulvermüller, 2007), lexico-semantic retrieval (Jobard, Crivello, & Tzourio-Mazoyer, 2003), and are part of a supramodal semantic network (Wirth et al., 2008). The occipital node of this connection subserves visual integration. Thus, an increased FC between these regions might reflect a functional reorganization that is characterized by supporting language comprehension using more sensory inputs. Moreover, this result indicated a reduced hemispheric functional specialization and perhaps an attempt to pool resources that are spared by the pathological developments in SD.

In comparison with AD and HC, SD patients showed a lower FC between the functional ROI encompassing the right fusiform/ parahippocampal gyri and the right inferior temporal pole. Disruption of this connection (no. 3) can be viewed as SD-typical, as the functional profile of the involved regions conforms to SD symptomatology. In particular, the right temporal pole is crucial for non-verbal (e.g., visual) object recognition, which is a hallmark impairment in SD associated with the loss of semantic knowledge (Mesulam, Thompson, Weintraub, & Rogalski, 2015; Nilakantan, Voss, Weintraub, Mesulam, & Rogalski, 2017). The right fusiform gyrus on the other hand is associated with working memory for faces, face perception, and non-verbal associative semantic knowledge (Brunyé, Moran, Holmes, Mahoney, & Taylor, 2017; Mion et al., 2010; Rangarajan et al., 2014), and the right parahippocampal gyrus is associated with working memory for object location as well as a function as an episodic buffer (Luck et al., 2010; Owen, Milner, Petrides, & Evans, 1996). In line with this, the patients with SD in the present study showed severe object recognition deficits assessed with BNT and oral picture-naming (table 1), even though no behavioral data about face perception or non-verbal semantic knowledge was available.

Similar to connection no. 3, FC was reduced in SD compared with AD and HC between the ROI comprised of left lingual/ intracalcarine/ precuneus cortex and the ROI including left posterior hippocampus/ thalamus (connection no. 4). This finding is in line with Seeley et al. (2009), who reported the medial temporal lobe as part of an SD-vulnerable network. Thus, in addition we showed a possible contribution of the primary visual (intracalcarine cortex), visual memory (lingual gyrus) and self-awareness (precuneus, i.e., default mode network) regions to that semantic network. It might appear surprising that the FC of the AD group was not significantly reduced in this connection, despite the commonly known medial temporal lobe atrophy and the pivotal role of the hippocampus in episodic memory encoding (La Joie et al., 2014; Tondelli et al., 2012). However, functional and anatomical changes do not necessarily overlap, and for instance, stable FC of the left hippocampus in early AD (except with right lateral prefrontal cortex) has been reported previously (L. Wang et al., 2006).

Lower FC in SD than in AD (and HC) was also found between the right lingual/ intracalcarine cortex and the left posterior hippocampus/ thalamus (connection no. 5). Therefore, connections between bilateral lingual gyri and the left hippocampus were detected in our HC sample (for illustration, see figure 3, connections no. 4 and 5), whereas either of them were damaged in SD, but not in AD. This supports the recent indication of a hippocampal contribution to the semantic memory network (La Joie et al., 2014). Because episodic memory is relatively spared in SD, the connections between the left posterior hippocampus and the bilateral lingual gyri might contribute to the semantic memory network. On the other hand, we did not find an expected decrease of FC in connection no. 4 in AD, although the precuneus and hippocampus contribute to episodic memory, which is typically impaired in AD. However, we have to bear in mind that our analysis was restricted to temporal lobe FC and thus did not cover the entire episodic memory network, including brain regions located in frontal and parietal lobes. In addition, no episodic memory data was available for the entire sample of our study. Future studies should investigate additional nodes from the aforementioned areas using larger sample sizes to tackle the increased number of connections and multiple testing correction that are associated with larger networks.

The only FC reduction common to both SD and AD compared with HC was found in connection no. 6. The functional role of the involved regions suggests an association with a frequently observed clinical presentation of AD and SD characterized by apathy and agitation, associated with the right orbitofrontal cortex (Bruen, McGeown, Shanks, & Venneri, 2008; Fernández-Matarrubia et al., 2018), and impairments in social behavior (SD only) related to the right anterior temporal lobe (Kumfor et al., 2016). Nonetheless, caution is advised with this interpretation, as we did not have data on social behavior or apathy/agitation of our patients. Regardless, we added a common pathway to the crossroad described by La Joie et al. (2014). They suggested that the hippocampus is a converging hub of an (AD-affected) episodic and a (SD-affected) semantic network. Accordingly, our data indicated that besides a shared damaged hub in AD and SD, the functional connection between the right anterior middle/ superior temporal gyri and the right orbitofrontal cortex might be a second candidate for the neuropathology shared in both clinical populations.

The final significant connection (no. 7) of the present study was found between the left orbitofrontal cortex and the left anterior inferior and middle temporal gyri. The literature suggests a functional role of this connection in deficient socioemotional abilities that are found predominantly in the behavioral variant of FTD (Dermody et al., 2016), and in higher level object representation, involving language and auditory processing. Unlike in connection no. 6, the AD group did not show an impaired FC of the orbitofrontal regions with the ipsilateral temporal cortex. Thus, one might speculate about a bilateral breakdown of orbitofrontal to temporal connections in SD, which might be related to the severity of the semantic deficit.

We also want to address some limitation of our study. Even though the overall sample size is large, the sample sizes of the three subgroups are considered small (16–23 individuals). Larger studies need to be conducted, however, this is especially challenging for SD given its low prevalence. Therefore, we pooled two SD samples from two different sites with different scanners; most individuals of the SD group were

from the Shanghai site. The data from different sites may have different noise levels such as thermal noise, physiological noise, and motion (Birn, 2012; Power et al., 2014). These artifacts are global in nature, and global signal regression (GRS) can successfully remove these and not only standardizes the data between sites, but also across individuals. That means the distribution of correlation coefficients is shifted from predominantly positive to mean zero with positive and negative coefficients. The negative correlations can appear as significant anti-correlations and need to be interpreted with caution, however, GRS can also improve the specificity of positive correlations (Murphy & Fox, 2017). Importantly, in this study, we do not interpret absolute negative correlations and solely compare *relative differences* in correlations between groups. Moreover, interpretation of group differences between AD and SD should take into account that the two dementia groups were not matched for disease stage (i.e., SD showed more severe deficits than AD).

To summarize the main findings of our study, the cohort of patients with SD yielded a number of distinct ipsilateral and contralateral connections of the temporal lobe that showed a significant reduction in FC. These connections included the regions on which our predictions were based on (i.e., hippocampus, fusiform gyrus, and temporal pole). Two functional connections were intriguing due to their distinctiveness from the other groups: the first was the connectivity breakdown between left posterior hippocampus and bilateral lingual gyri, likely reflecting the neuronal underpinning of semantic memory loss. Second, a bilateral disruption of connectivity between temporal and frontal lobes was found. This aligns well with the pathophysiology within the FTD spectrum and especially with SD.

FC in AD was relatively intact compared to SD, which contradicted our hypothesis. The only connection with significantly reduced FC encompassed the right orbitofrontal cortex and the right anterior temporal lobe (no. 6), which we identified as an AD/SD-common pathway. Additionally, figure 2 illustrates that our AD group had a lower FC than the HC in connections no. 1, 2, and to a smaller extent no. 5 which all missed significance. These FC signatures in the AD group could be attributed to their mild stage of symptom progression (MMSE of 24.5), and potentially an early marker of the disease, but larger and longitudinal studies are needed.

Following the "cortically distributed plus semantic hub" theory, several connections were found to be significantly altered in the present study, which affected the anterior temporal lobe – semantic hub – regions (no. 1, 3, 6, and 7). Moreover, their counterparts were partly localized in the modality-specific regions described by Patterson et al. (2007), but also in orbitofrontal regions. This agreement of our results with the arguments in Patterson et al. (2007) supported the "distributed plus hub" theory, because we found altered FC in connections between the hub and the modality-specific regions. Taken together, the present study particularly contributed to the understanding of distinct pathophysiological changes in AD and SD that are related to disruptions of functional networks in the temporal lobe. The unique aspect of our study was the definition of ROIs based on functional brain segregation rather than anatomy for FC

analysis. Due to the comparably strict statistical approach and the predefined choice of ROIs, our study provided a fine-grained overview of FC aberration related to temporal lobe function in AD and SD.

Data Availability

Raw imaging data can be requested from the corresponding author. Aggregated data and analysis scripts to generate all results and figures is available at OSF (https://osf.io/t4jnv/).

Funding

This work was supported by the Swedish Alzheimerfonden, the Swiss Synapsis Foundation, and the University of Bern, the Beijing Natural Science Foundation (7182088), and the NSFC (31872785). Simon Schwab acknowledges funding from the Swiss National Science Foundation (SNSF, No. 162066 and 171598).

References

Afyouni, S., & Nichols, T. E. (2018). Insight and inference for DVARS. *NeuroImage*, *172*, 291–312.

Agosta, F., Galantucci, S., Valsasina, P., Canu, E., Meani, A., Marcone, A., … Filippi, M. (2014). Disrupted brain connectome in semantic variant of primary progressive aphasia. *Neurobiology of Aging*, *35*(11), 2646–2655.

Allen, G., Barnard, H., McColl, R., Hester, A. L., Fields, J. A., Weiner, M. F., … Cullum, C. M. (2007). Reduced hippocampal functional connectivity in Alzheimer disease. *Archives of Neurology*, *64*(10), 1482–1487.

Andreotti, J., Dierks, T., Wahlund, L.-O., & Grieder, M. (2017). Diverging Progression of Network Disruption and Atrophy in Alzheimer's Disease and Semantic Dementia. *Journal of Alzheimer's Disease: JAD*, *55*(3), 981–993.

Ashburner, J., & Friston, K. J. (2000). Voxel-Based Morphometry—The Methods. *NeuroImage*, *11*(6), 805–821.

Birn, R. M. (2012). The role of physiological noise in resting-state functional connectivity. *NeuroImage*, *62*(2), 864–870.

Biswal, B., Yetkin, F. Z., Haughton, V. M., & Hyde, J. S. (1995). Functional connectivity in the motor cortex of resting human brain using echo-planar MRI. *Magnetic Resonance in Medicine: Official Journal of the Society of Magnetic Resonance in Medicine / Society of Magnetic Resonance in Medicine*, *34*(4), 537–541.

Blackwell, A. D., Sahakian, B. J., Vesey, R., Semple, J. M., Robbins, T. W., & Hodges, J. R. (2004). Detecting dementia: novel neuropsychological markers of preclinical Alzheimer's disease. *Dementia and Geriatric Cognitive Disorders*, *17*(1-2), 42–48.

Bozeat, S., Lambon Ralph, M. A., Patterson, K., Garrard, P., & Hodges, J. R. (2000). Non-verbal semantic impairment in semantic dementia. *Neuropsychologia*, *38*(9), 1207–1215.

Brier, M. R., Thomas, J. B., Snyder, A. Z., Benzinger, T. L., Zhang, D., Raichle, M. E., … Ances, B. M. (2012). Loss of intranetwork and internetwork resting state functional connections with Alzheimer's disease progression. *The Journal of Neuroscience: The Official Journal of the Society for Neuroscience*, *32*(26), 8890–8899.

Broyd, S. J., Demanuele, C., Debener, S., Helps, S. K., James, C. J., & Sonuga-Barke, E. J. S. (2009). Default-mode brain dysfunction in mental disorders: a systematic review. *Neuroscience and Biobehavioral Reviews*, *33*(3), 279–296.

Bruen, P. D., McGeown, W. J., Shanks, M. F., & Venneri, A. (2008). Neuroanatomical correlates of neuropsychiatric symptoms in Alzheimer's disease. *Brain: A Journal of Neurology*, *131*(Pt 9), 2455–2463.

Brunyé, T. T., Moran, J. M., Holmes, A., Mahoney, C. R., & Taylor, H. A. (2017). Non-invasive brain stimulation targeting the right fusiform gyrus selectively increases working memory for faces. *Brain*

and Cognition, *113*, 32–39.

Buckner, R. L., Snyder, A. Z., Shannon, B. J., LaRossa, G., Sachs, R., Fotenos, A. F., … Mintun, M. A. (2005). Molecular, structural, and functional characterization of Alzheimer's disease: evidence for a relationship between default activity, amyloid, and memory. *The Journal of Neuroscience: The Official Journal of the Society for Neuroscience*, *25*(34), 7709–7717.

Burianova, H., McIntosh, A. R., & Grady, C. L. (2010). A common functional brain network for autobiographical, episodic, and semantic memory retrieval. *NeuroImage*, *49*(1), 865–874.

Chang, C., & Glover, G. H. (2009). Effects of model-based physiological noise correction on default mode network anti-correlations and correlations. *NeuroImage*, *47*(4), 1448–1459.

Chen, Y., Chen, K., Ding, J., Zhang, Y., Yang, Q., Lv, Y., … Han, Z. (2017). Brain Network for the Core Deficits of Semantic Dementia: A Neural Network Connectivity-Behavior Mapping Study. *Frontiers in Human Neuroscience*, *11*, 267.

Collins, J. A., Montal, V., Hochberg, D., Quimby, M., Mandelli, M. L., Makris, N., … Dickerson, B. C. (2017). Focal temporal pole atrophy and network degeneration in semantic variant primary progressive aphasia. *Brain: A Journal of Neurology*, *140*(2), 457–471.

Craddock, R. C., James, G. A., Holtzheimer, P. E., 3rd, Hu, X. P., & Mayberg, H. S. (2012). A whole brain fMRI atlas generated via spatially constrained spectral clustering. *Human Brain Mapping*, *33*(8), 1914–1928.

Dermody, N., Wong, S., Ahmed, R., Piguet, O., Hodges, J. R., & Irish, M. (2016). Uncovering the Neural Bases of Cognitive and Affective Empathy Deficits in Alzheimer's Disease and the Behavioral-Variant of Frontotemporal Dementia. *Journal of Alzheimer's Disease: JAD*, *53*(3), 801–816.

Ding, J., Chen, K., Chen, Y., Fang, Y., Yang, Q., Lv, Y., … Han, Z. (2016). The Left Fusiform Gyrus is a Critical Region Contributing to the Core Behavioral Profile of Semantic Dementia. *Frontiers in Human Neuroscience*, *10*, 215.

Duss, S. B., Reber, T. P., Hänggi, J., Schwab, S., Wiest, R., Müri, R. M., … Henke, K. (2014). Unconscious relational encoding depends on hippocampus. *Brain: A Journal of Neurology*, *137*(Pt 12), 3355–3370.

Farb, N. A. S., Grady, C. L., Strother, S., Tang-Wai, D. F., Masellis, M., Black, S., … Chow, T. W. (2013). Abnormal network connectivity in frontotemporal dementia: evidence for prefrontal isolation. *Cortex; a Journal Devoted to the Study of the Nervous System and Behavior*, *49*(7), 1856–1873.

Fernández-Matarrubia, M., Matías-Guiu, J. A., Cabrera-Martín, M. N., Moreno-Ramos, T., Valles-Salgado, M., Carreras, J. L., & Matías-Guiu, J. (2018). Different apathy clinical profile and neural correlates in behavioral variant frontotemporal dementia and Alzheimer's disease. *International Journal of Geriatric Psychiatry*, *33*(1), 141–150.

Fox, M. D., & Raichle, M. E. (2007). Spontaneous fluctuations in brain activity observed with functional magnetic resonance imaging. *Nature Reviews. Neuroscience*, *8*(9), 700–711.

Friston, K. J., Ashburner, J. T., Kiebel, S. J., Penny, W. D., & Nichols, T. E. (2007). *Statistical Parametric*

Mapping: The Analysis of Functional Brain Images (Vol. 8, p. 647). Elsevier Science.

Gaser, C., & Dahnke, R. (2016). CAT-a computational anatomy toolbox for the analysis of structural MRI data. *HBM*, *2016*, 336–348.

Gorno-Tempini, M. L., Hillis, A. E., Weintraub, S., Kertesz, A., Mendez, M., Cappa, S. F., … Grossman, M. (2011). Classification of primary progressive aphasia and its variants. *Neurology*, *76*(11), 1006–1014.

Greicius, M. D., Srivastava, G., Reiss, A. L., & Menon, V. (2004). Default-mode network activity distinguishes Alzheimer's disease from healthy aging: evidence from functional MRI. *Proceedings of the National Academy of Sciences of the United States of America*, *101*(13), 4637–4642.

Grieder, M., Crinelli, R. M., Jann, K., Federspiel, A., Wirth, M., Koenig, T., … Dierks, T. (2013). Correlation between topographic N400 anomalies and reduced cerebral blood flow in the anterior temporal lobes of patients with dementia. *Journal of Alzheimer's Disease: JAD*, *36*(4), 711–731.

Guo, C. C., Gorno-Tempini, M. L., Gesierich, B., Henry, M., Trujillo, A., Shany-Ur, T., … Seeley, W. W. (2013). Anterior temporal lobe degeneration produces widespread network-driven dysfunction. *Brain: A Journal of Neurology*, *136*(Pt 10), 2979–2991.

Henke, K. (2010). A model for memory systems based on processing modes rather than consciousness. *Nature Reviews. Neuroscience*, *11*(7), 523–532.

Hodges, J. R., & Patterson, K. (2007). Semantic dementia: a unique clinicopathological syndrome. *Lancet Neurology*, *6*(11), 1004–1014.

Hurley, R. S., Bonakdarpour, B., Wang, X., & Mesulam, M.-M. (2015). Asymmetric connectivity between the anterior temporal lobe and the language network. *Journal of Cognitive Neuroscience*, *27*(3), 464–473.

Irish, M., Bunk, S., Tu, S., Kamminga, J., Hodges, J. R., Hornberger, M., & Piguet, O. (2016). Preservation of episodic memory in semantic dementia: The importance of regions beyond the medial temporal lobes. *Neuropsychologia*, *81*, 50–60.

Jobard, G., Crivello, F., & Tzourio-Mazoyer, N. (2003). Evaluation of the dual route theory of reading: a metanalysis of 35 neuroimaging studies. *NeuroImage*, *20*(2), 693–712.

Kobeleva, X., Firbank, M., Peraza, L., Gallagher, P., Thomas, A., Burn, D. J., … Taylor, J.-P. (2017). Divergent functional connectivity during attentional processing in Lewy body dementia and Alzheimer's disease. *Cortex; a Journal Devoted to the Study of the Nervous System and Behavior*, *92*, 8–18.

Kumfor, F., Landin-Romero, R., Devenney, E., Hutchings, R., Grasso, R., Hodges, J. R., & Piguet, O. (2016). On the right side? A longitudinal study of left- versus right-lateralized semantic dementia. *Brain: A Journal of Neurology*, *139*(Pt 3), 986–998.

La Joie, R., Landeau, B., Perrotin, A., Bejanin, A., Egret, S., Pélerin, A., … Chételat, G. (2014). Intrinsic connectivity identifies the hippocampus as a main crossroad between Alzheimer's and semantic dementia-targeted networks. *Neuron*, *81*(6), 1417–1428.

Landin-Romero, R., Tan, R., Hodges, J. R., & Kumfor, F. (2016). An update on semantic dementia: genetics, imaging, and pathology. *Alzheimer's Research & Therapy*, *8*(1), 52.

Liu, J., Zhang, X., Yu, C., Duan, Y., Zhuo, J., Cui, Y., … Liu, Y. (2016). Impaired Parahippocampus Connectivity in Mild Cognitive Impairment and Alzheimer's Disease. *Journal of Alzheimer's Disease: JAD*, *49*(4), 1051–1064.

Luck, D., Danion, J.-M., Marrer, C., Pham, B.-T., Gounot, D., & Foucher, J. (2010). The right parahippocampal gyrus contributes to the formation and maintenance of bound information in working memory. *Brain and Cognition*, *72*(2), 255–263.

Margulies, D. S., Kelly, A. M. C., Uddin, L. Q., Biswal, B. B., Castellanos, F. X., & Milham, M. P. (2007). Mapping the functional connectivity of anterior cingulate cortex. *NeuroImage*, *37*(2), 579–588.

Mascali, D., DiNuzzo, M., Serra, L., Mangia, S., Maraviglia, B., Bozzali, M., & Giove, F. (2018). Disruption of Semantic Network in Mild Alzheimer's Disease Revealed by Resting-State fMRI. *Neuroscience*, *371*, 38–48.

McClelland, J. L., & Rogers, T. T. (2003). The parallel distributed processing approach to semantic cognition. *Nature Reviews. Neuroscience*, *4*(4), 310–322.

McDonough, I. M., & Nashiro, K. (2014). Network complexity as a measure of information processing across resting-state networks: evidence from the Human Connectome Project. *Frontiers in Human Neuroscience*, *8*, 409.

Mesulam, M.-M., Thompson, C. K., Weintraub, S., & Rogalski, E. J. (2015). The Wernicke conundrum and the anatomy of language comprehension in primary progressive aphasia. *Brain: A Journal of Neurology*, *138*(Pt 8), 2423–2437.

Mion, M., Patterson, K., Acosta-Cabronero, J., Pengas, G., Izquierdo-Garcia, D., Hong, Y. T., … Nestor, P. J. (2010). What the left and right anterior fusiform gyri tell us about semantic memory. *Brain: A Journal of Neurology*, *133*(11), 3256–3268.

Mummery, C. J., Patterson, K., Price, C. J., Ashburner, J., Frackowiak, R. S., & Hodges, J. R. (2000). A voxel-based morphometry study of semantic dementia: relationship between temporal lobe atrophy and semantic memory. *Annals of Neurology*, *47*(1), 36–45.

Murphy, K., & Fox, M. D. (2017). Towards a consensus regarding global signal regression for resting state functional connectivity MRI. *NeuroImage*, *154*, 169–173.

Neary, D., Snowden, J. S., Gustafson, L., Passant, U., Stuss, D., Black, S., … Benson, D. F. (1998). Frontotemporal lobar degeneration: a consensus on clinical diagnostic criteria. *Neurology*, *51*(6), 1546–1554.

Nilakantan, A. S., Voss, J. L., Weintraub, S., Mesulam, M.-M., & Rogalski, E. J. (2017). Selective verbal recognition memory impairments are associated with atrophy of the language network in non-semantic variants of primary progressive aphasia. *Neuropsychologia*, *100*, 10–17.

Orban, P., Dansereau, C., Desbois, L., Mongeau-Pérusse, V., Giguère, C.-É., Nguyen, H., … Bellec, P. (2018). Multisite generalizability of schizophrenia diagnosis classification based on functional brain connectivity. *Schizophrenia Research*, *192*, 167–171.

Owen, A. M., Milner, B., Petrides, M., & Evans, A. C. (1996). A specific role for the right parahippocampal gyrus in the retrieval of object-location: a positron emission tomography study. *Journal of Cognitive Neuroscience*, *8*(6), 588–602.

Patterson, K., Nestor, P. J., & Rogers, T. T. (2007). Where do you know what you know? The representation of semantic knowledge in the human brain. *Nature Reviews. Neuroscience*, *8*(12), 976–987.

Poulin, S. P., Dautoff, R., Morris, J. C., Barrett, L. F., Dickerson, B. C., & Alzheimer's Disease Neuroimaging Initiative. (2011). Amygdala atrophy is prominent in early Alzheimer's disease and relates to symptom severity. *Psychiatry Research*, *194*(1), 7–13.

Power, J. D., Barnes, K. A., Snyder, A. Z., Schlaggar, B. L., & Petersen, S. E. (2012). Spurious but systematic correlations in functional connectivity MRI networks arise from subject motion. *NeuroImage*, *59*(3), 2142–2154.

Power, J. D., Mitra, A., Laumann, T. O., Snyder, A. Z., Schlaggar, B. L., & Petersen, S. E. (2014). Methods to detect, characterize, and remove motion artifact in resting state fMRI. *NeuroImage*, *84*, 320–341.

Raichle, M. E., MacLeod, A. M., Snyder, A. Z., Powers, W. J., Gusnard, D. A., & Shulman, G. L. (2001). A default mode of brain function. *Proceedings of the National Academy of Sciences of the United States of America*, *98*(2), 676–682.

Rangarajan, V., Hermes, D., Foster, B. L., Weiner, K. S., Jacques, C., Grill-Spector, K., & Parvizi, J. (2014). Electrical stimulation of the left and right human fusiform gyrus causes different effects in conscious face perception. *The Journal of Neuroscience: The Official Journal of the Society for Neuroscience*, *34*(38), 12828–12836.

Reijmer, Y. D., Leemans, A., Caeyenberghs, K., Heringa, S. M., Koek, H. L., Biessels, G. J., & Utrecht Vascular Cognitive Impairment Study Group. (2013). Disruption of cerebral networks and cognitive impairment in Alzheimer disease. *Neurology*, *80*(15), 1370–1377.

Seeley, W. W., Crawford, R. K., Zhou, J., Miller, B. L., & Greicius, M. D. (2009). Neurodegenerative diseases target large-scale human brain networks. *Neuron*, *62*(1), 42–52.

Shtyrov, Y., & Pulvermüller, F. (2007). Early MEG activation dynamics in the left temporal and inferior frontal cortex reflect semantic context integration. *Journal of Cognitive Neuroscience*, *19*(10), 1633–1642.

Smith, S. M., Vidaurre, D., Beckmann, C. F., Glasser, M. F., Jenkinson, M., Miller, K. L., … Van Essen, D. C. (2013). Functional connectomics from resting-state fMRI. *Trends in Cognitive Sciences*, *17*(12), 666–682.

Sormaz, M., Jefferies, E., Bernhardt, B. C., Karapanagiotidis, T., Mollo, G., Bernasconi, N., … Smallwood, J. (2017). Knowing what from where: Hippocampal connectivity with temporoparietal cortex at rest is linked to individual differences in semantic and topographic memory. *NeuroImage*, *152*, 400–410.

Tahmasian, M., Pasquini, L., Scherr, M., Meng, C., Förster, S., Mulej Bratec, S., … Drzezga, A. (2015). The lower hippocampus global connectivity, the higher its local metabolism in Alzheimer disease. *Neurology*, *84*(19), 1956–1963.

Tijms, B. M., Yeung, H. M., Sikkes, S. A. M., Möller, C., Smits, L. L., Stam, C. J., … Barkhof, F. (2014). Single-subject gray matter graph properties and their relationship with cognitive impairment in early- and late-onset Alzheimer's disease. *Brain Connectivity*, *4*(5), 337–346.

Tondelli, M., Wilcock, G. K., Nichelli, P., De Jager, C. A., Jenkinson, M., & Zamboni, G. (2012). Structural MRI changes detectable up to ten years before clinical Alzheimer's disease. *Neurobiology of Aging*, *33*(4), 825.e25–e36.

Tulving, E. (1983). *Elements of Episodic Memory*. Oxford: Oxford University Press.

Villain, N., Fouquet, M., Baron, J.-C., Mézenge, F., Landeau, B., de La Sayette, V., … Chételat, G. (2010). Sequential relationships between grey matter and white matter atrophy and brain metabolic abnormalities in early Alzheimer's disease. *Brain: A Journal of Neurology*, *133*(11), 3301–3314.

Vogel, A., Gade, A., Stokholm, J., & Waldemar, G. (2005). Semantic memory impairment in the earliest phases of Alzheimer's disease. *Dementia and Geriatric Cognitive Disorders*, *19*(2-3), 75–81.

Wang, J., Zuo, X., Dai, Z., Xia, M., Zhao, Z., Zhao, X., … He, Y. (2013). Disrupted functional brain connectome in individuals at risk for Alzheimer's disease. *Biological Psychiatry*, *73*(5), 472–481.

Wang, L., Zang, Y., He, Y., Liang, M., Zhang, X., Tian, L., … Li, K. (2006). Changes in hippocampal connectivity in the early stages of Alzheimer's disease: evidence from resting state fMRI. *NeuroImage*, *31*(2), 496–504.

Wirth, M., Horn, H., Koenig, T., Razafimandimby, A., Stein, M., Mueller, T., … Strik, W. (2008). The early context effect reflects activity in the temporo-prefrontal semantic system: evidence from electrical neuroimaging of abstract and concrete word reading. *NeuroImage*, *42*(1), 423–436.

Zhang, D., & Raichle, M. E. (2010). Disease and the brain's dark energy. *Nature Reviews. Neurology*, *6*(1), 15–28.

Figures

Figure 1

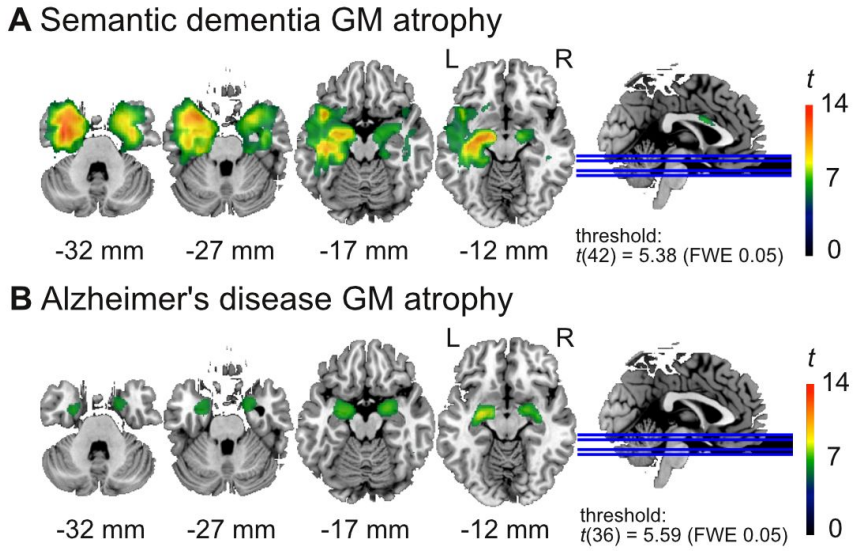

Figure 1: Gray matter (GM) atrophy in **(A)** the semantic dementia (SD) patients (n = 24) and **(B)** Alzheimer's disease (AD) patients (n = 18) compared to the healthy elderly control group (n = 20). The AD patients show atrophy in the amygdala, while the SD patients have atrophy in larger areas of the left anterior temporal cortex including the temporal pole.

Figure 2

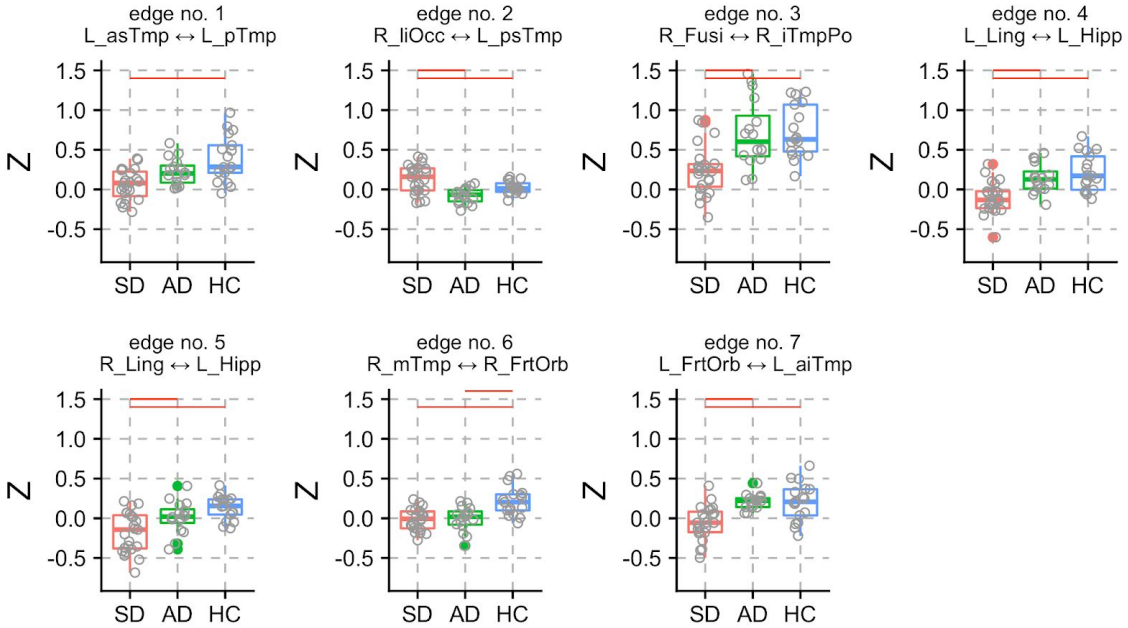

Figure 2: Z-scores of seven connections (edges 1–7) with significant group differences. Post-hoc tests between the three groups were performed, and significant group differences are denoted with red horizontal lines (see table 2 for a detailed description of the regions). Grey circles represent single subject data points. Solid circles represent outliers.

Figure 3

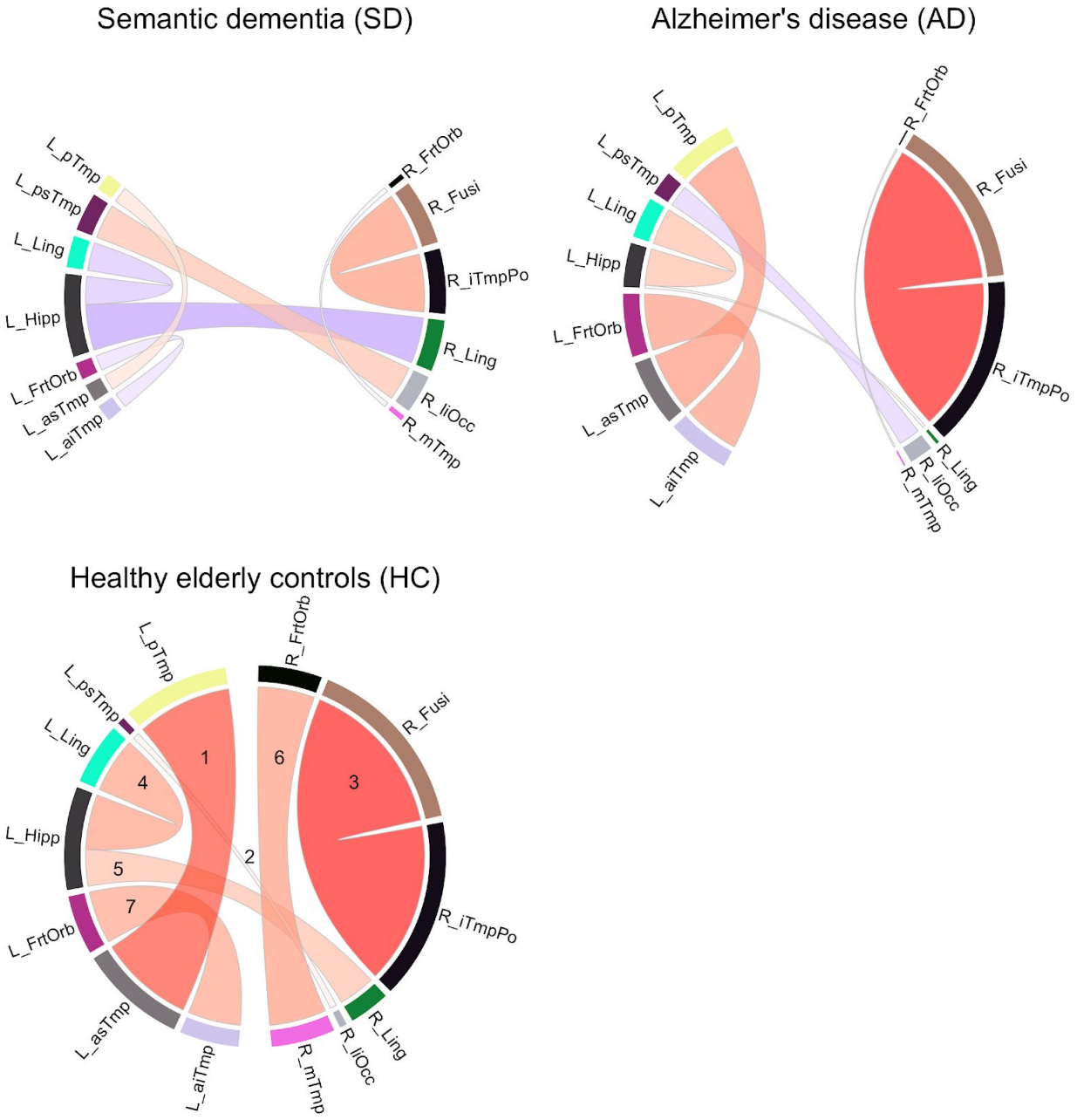

Figure 3: Functional connectivity (FC) strengths (Z-values) of the three groups. Color shades and thickness of the links are proportional to FC strengths; shades of red reflect positive, shades of blue negative strengths. Numbers in HC group indicate edge numbers (see table 2 for a detailed description of the regions).

Tables

Table 1

Table 1. Descriptives and clinical scores. The non-parametric Kruskal-Wallis-Test was run to assess statistically relevant differences over all three groups (not depicted in the table). All clinical scores that were available for all three groups (i.e., MMSE, BNT, lexical decision, AF, VF) yielded a *p*-value of 0.001 or below. A significant age effect was found (H= 10.8, df = 2, p = 0.004), but no effect of education. Group-wise post-hoc comparisons were performed using the non-parametric Kolmogorov-Smirnov-Test. Note that in the SD group, education, BNT, lexical decision, AF, and VF scores were only available from the Stockholm site (statistics in italics). In contrast, scores of oral picture-naming and word-triple association were only available from the Shanghai site. Age, gender, and MMSE were available from both sites (statistics in bold).

	HC (n=17)	AD (n=16)	SD (n=23)	
	Mean (st.dev.)	Mean (st.dev.)	Mean (st.dev.)	p-value
Age, years	67.9 (3.3)	68.4 (8.5)	**61.5 (7.4)**	0.004
Gender (F:M)	12:5	7:9	**10:13**	-
Education, years	13.9 (3.1)	13.1 (3.0)	*12.4 (1.5)*	0.61
CDS	-	1.0 (1.0)	*1.8 (2.2)*	0.60
GDS	-	2.9 (0.8)	*3.8 (0.4)*	0.031
MMSE (max 30)	28.8 (0.8)	24.5 (4.8)	**20.8 (5.2)**[1]	< 0.0001
BNT (% of max 60)	90.7 (6.1)	76.0 (1.1)	*13.7 (9.5)*	< 0.0001
Oral picture-naming (% of max 140)	-	-	28.5 (19.1)	-
Word-triple association (% of max 70)	-	-	72.7 (14.0)	-
Lexical decision (% of max 352)	98.4 (1.0)[2]	94.9 (6.5)[2]	*92.4 (6.5)*[2]	0.002
AF, animals/minute	23.8 (5.9)	14.1 (4.2)	*5.6 (4.3)*	< 0.0001
VF, verbs/minute	21.9 (5.8)	11.9 (5.0)	*7.0 (2.8)*	< 0.0001

[1] SD = 19; [2] HC = 16, AD = 12, SD = 4. Abbreviations: CDS = Cornell Depression Scale; GDS = Global Deterioration Scale; MMSE = Mini-Mental State Examination; BNT = Boston Naming Test; AF = animal fluency; VF = verb fluency.

Table 2

Table 2. Seven functional connections that demonstrated significant group differences. Connections are sorted according their F-value.

Edge no.	Node no.	Node no.	Region	Region	*F*-value	FDR adj. *p*-value
4	70	37	Left lingual gyrus / intracalcarine cortex / precuneus cortex	Left posterior hippocampus / thalamus	12.94	0.03
3	198	32	Right fusiform cortex / parahippocampal gyrus	Right inferior temporal pole	12.45	0.03
6	153	71	Right anterior middle temporal gyrus / superior temporal gyrus	Right orbitofrontal cortex	12.25	0.03
7	112	72	Left orbitofrontal cortex / insular cortex	Left anterior inferior temporal gyrus / middle temporal gyrus	11.88	0.03
2	85	24	Right lateral inferior occipital cortex / lateral superior occipital cortex	Left posterior superior temporal gyrus / central opercular cortex / parietal opercular cortex / planum temporale	11.3	0.036
1	129	11	Left anterior superior temporal gyrus / middle temporal gyrus / insular cortex	Left posterior middle temporal gyrus / superior temporal gyrus	11.02	0.037
5	89	37	Right lingual gyrus / intracalcarine cortex	Left posterior hippocampus / thalamus	10.74	0.038

Table 3

Table 3. Post-hoc Tukey HSD p-values for the three single comparisons (rows) and for each of the seven node-pairs that had a significant group effect (columns). Significant values reflect that the group effect was driven by a specific group level contrast. Lowest *p*-value per edge highlighted in bold.

Edge No.	1	2	3	4	5	6	7
AD vs HC	0.098	0.082	0.98	0.54	0.22	0.0005	1.00
SD vs HC	**<0.0001**	0.044	**0.0002**	**<0.0001**	**<0.0001**	**<0.0001**	**0.0004**
SD vs AD	0.064	**<0.0001**	0.0004	0.002	0.024	0.97	**0.0004**

Supplementary

Supplementary Figure 1

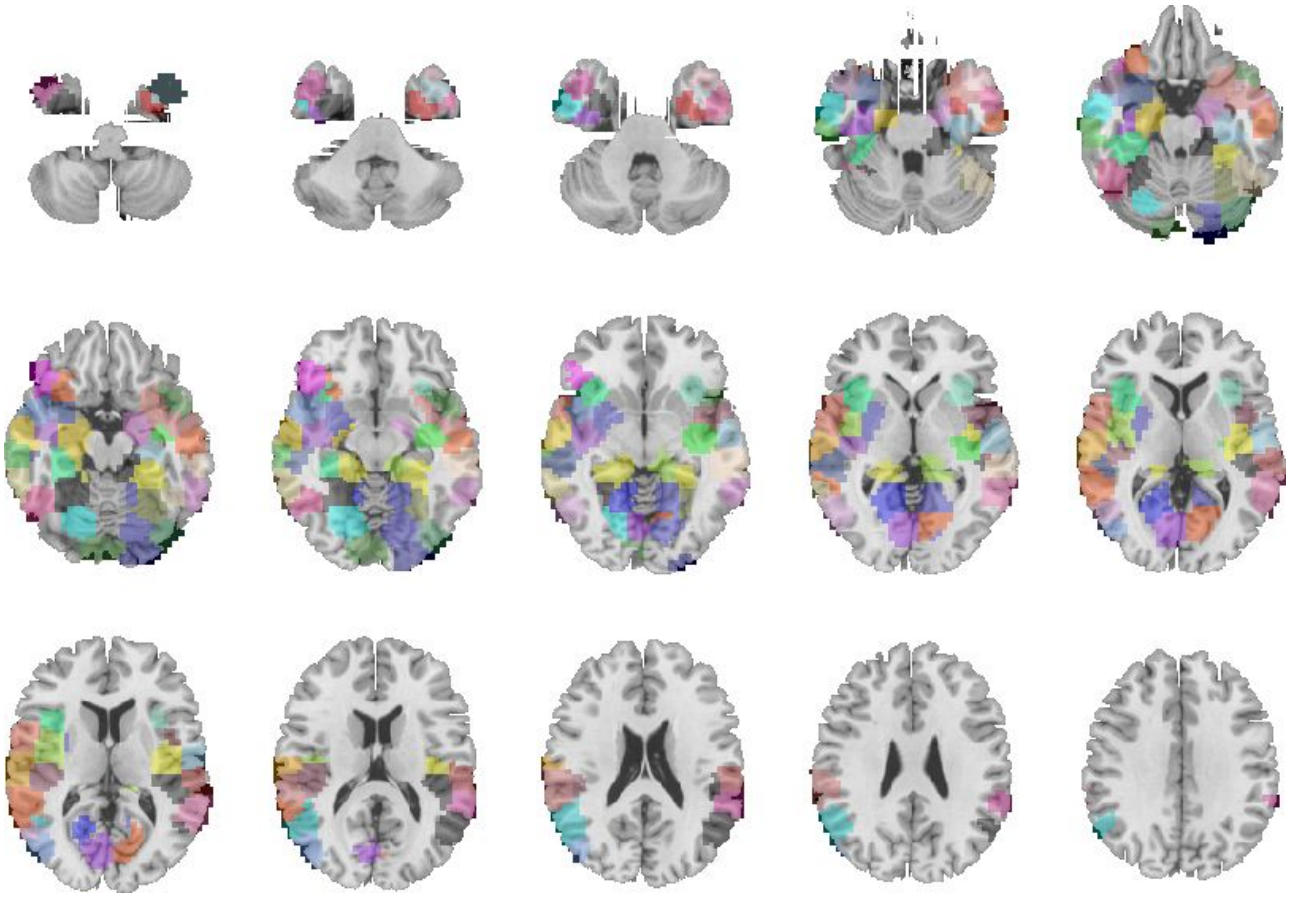

Supplementary Figure 1. Sixty-six nodes from a functional parcellation by Craddock (2012) (*k* = 200) that were selected based on their overlap with structures in the temporal cortex, the hippocampus, and the amygdala.